PHOTONICS Research

Ultrabroadband, few-cycle pulses directly from a Mamyshev fiber oscillator

CHUNYANG MA,[1,2] ANKITA KHANOLKAR,[3] YIMIN ZANG,[3] AND ANDY CHONG[2,3,*]

[1]Department of Electronic Science and Engineering, Jilin University, Changchun 130012, China
[2]Department of Physics, University of Dayton, Dayton, Ohio 45469, USA
[3]Department of Electro-Optics and Photonics, University of Dayton, Dayton, Ohio 45469, USA
*Corresponding author: achong1@udayton.edu

Received 13 September 2019; revised 12 November 2019; accepted 13 November 2019; posted 15 November 2019 (Doc. ID 377733); published 20 December 2019

While the performance of mode-locked fiber lasers has been improved significantly, the limited gain bandwidth restricts them from generating ultrashort pulses approaching a few cycles or even shorter. Here we present a novel method to achieve few-cycle pulses (∼5 cycles) with an ultrabroad spectrum (∼400 nm at −20 dB) from a Mamyshev oscillator configuration by inserting a highly nonlinear photonic crystal fiber and a dispersion delay line into the cavity. A dramatic intracavity spectral broadening can be stabilized by the unique nonlinear processes of a self-similar evolution as a nonlinear attractor in the gain fiber and a "perfect" saturable absorber action of the Mamyshev oscillator. To the best of our knowledge, this is the shortest pulse width and broadest spectrum directly generated from a fiber laser.

https://doi.org/10.1364/PRJ.8.000065

1. INTRODUCTION

Ultrashort pulses with high peak power have enabled numerous applications in various fields including nonlinear microscopy [1], materials processing [2], sensing [3], femtochemistry [4], frequency comb [5,6], etc. Particularly, optical pulses of temporal durations reaching few cycles or a single cycle of the carrier frequency with spectra broader than an octave spanning have been essential for a variety of cutting-edge applications such as attosecond science [7,8], high-harmonic generation [9], and coherent X-ray generation [10]. Currently, solid-state lasers have been the forefront of few-cycle pulse generation owing to their broad gain bandwidths (BWs) [11–13]. Even though the performance of fiber lasers has been comparable to solid-state lasers in terms of pulse energies and peak powers, generating few-cycle or single-cycle pulses is still challenging for fiber lasers because of their limited gain BW.

One general method to obtain few-cycle pulses from fiber lasers is using nonlinear pulse compression outside the cavity [14–16]. Another attractive method to generate a single-cycle pulse from a fiber device is by coherently combining two supercontinuum spectra from highly nonlinear photonic crystal fibers (PCF) [17]. However, these devices are extremely complex with stability issues. On the other hand, ultrashort pulses with broad spectra generated directly from mode-locked fiber lasers have advantages. Pulses generated directly from a laser are more stable with less noise since the temporal phase on a pulse is reshaped for each round trip. Furthermore, pulses can be conveniently compressed externally for even shorter pulse durations. Therefore, it is strongly desirable to generate broad spectra beyond the gain BW from a simple fiber oscillator.

In order to generate a broad spectrum directly from a fiber oscillator, a proper fiber laser design is crucial to permit a substantial intracavity spectral broadening without losing the mode-locked operation. It turns out that a recently discovered fiber laser operation facilitates such a broad mode-locked spectrum. In 2010, a self-similar pulse evolution was demonstrated in mode-locked fiber lasers [18–20]. Self-similar pulses are linearly chirped parabolic pulses as asymptotic solutions of a normal group velocity dispersion (GVD) fiber amplifier [21]. Remarkably, a self-similar pulse is a strong nonlinear attractor of the gain fiber. Even though a strong perturbation such as a substantial accumulation of nonlinear phase is introduced, the perturbed pulse conveniently returns to a self-similar parabolic pulse by strong filtering followed by a normal GVD fiber amplifier [22]. As a consequence, an enormous intracavity spectral broadening can be stabilized as a mode-locked operation by strong spectral filtering and self-similar amplification. By inserting a highly nonlinear PCF after the self-similar pulse is established in the gain fiber, a very broad spectrum (∼200 nm BW), which is much larger than the gain BW, has been demonstrated [23]. Pulses from the laser are highly chirped but could be dechirped externally to ∼20 fs. Since then, there has not been much improvement in the pulse duration from fiber lasers.

In Ref. [23], a chirped parabolic pulse was coupled into PCF; therefore, the broadened spectral BW was limited. Recently performed simulations proved that a huge spectral broadening can occur by dechirping these chirped parabolic pulses before they enter PCF with the help of an intracavity dispersion delay line (DDL) [24]. These simulations yielded broad spectra only when an ideal saturable absorber with ~100% modulation depth was used. However, such broad spectra have not been observed in experiments. One conjecture for this discrepancy is the nonideal saturable absorber in lasers. The subsequent experiments and numerical studies suggested that the saturable absorber in fiber lasers must be improved to stabilize substantial spectral broadening.

In 2017, a unique fiber laser cavity called Mamyshev oscillator was demonstrated [25]. A Mamyshev oscillator exhibits a transmission–intensity curve that jumps from zero to maximum like a step function at a certain intensity, which is referred to as a "perfect" saturable absorber [26]. This oscillator has successfully demonstrated its potential for high pulse energies (50 nJ) and short pulse (40 fs) durations [25]. Lately, the same oscillator with a large-core PCF design has achieved a remarkable performance of 1 μJ pulse energy and 40 fs pulse duration [27]. Owing to its unique "perfect" saturable absorbing action, the Mamyshev oscillator appears to be a good candidate to stabilize a massive intracavity spectrum broadening.

Here, we present the generation of few-cycle pulses directly from a mode-locked Mamyshev fiber oscillator. To enhance the intracavity spectral BW, a DDL followed by a highly nonlinear PCF was inserted in the cavity. A very broad mode-locked spectrum (~400 nm at −20 dB) with 5-cycle pulse duration (17 fs) is generated. It is noteworthy that this broad spectrum can be mode-locked owing to the nonlinear processes of a "perfect" saturable absorber and the self-similar evolution.

2. EXPERIMENTS

The experimental setup of the Mamyshev oscillator is schematically illustrated in Fig. 1. The oscillator consists of two arms. In each arm, a pump combiner couples a 976 nm pump into a 3.1 m Yb-doped double cladding gain fiber (Nufern, SM-YDF-5/130-VIII), which is followed by a 0.7 m single-mode fiber (SMF). Including SMFs before gain fibers, the total fiber cavity length is 9 m, which corresponds to the total cavity GVD of 0.146 ps^2. Two free space isolators ensure a unidirectional laser operation. Two 600 lines/mm gratings with collimators serve as narrow 4 nm BW Gaussian spectral filters centered at ~1040 nm and ~1050 nm wavelength while the center wavelength of the laser is at ~1045 nm. Two half-wave plates (HWPs) after the isolators adjust the polarization to maximize diffraction efficiency of the diffraction grating.

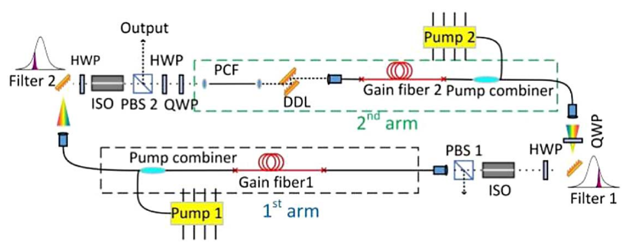

Fig. 1. Schematic of the Mamyshev fiber oscillator. PBS, polarizing beam splitter; HWP, half-wave plate; QWP, quarter-wave plate; ISO, free space isolator; DDL, dispersion delay line (a grating pair); PCF, photonic crystal fiber.

The first arm is used to ensure self-similar operation in the gain fiber. However, an anomalous DDL in the form of a 1000 lines/mm grating pair is inserted in the second arm to compress the self-similar pulse established in the gain fiber. The compressed pulse is coupled into 45 cm of an all-normal dispersion (ANDi) PCF with a small positive GVD and a very small mode field diameter (MFD) of 3 μm. In the second arm, two quarter-wave plates (QWPs), an HWP, and a polarization beam splitter (PBS) serve as a nonlinear polarization evolution (NPE)-based artificial saturable absorber to start mode-locking. Once the laser is mode-locked by adjusting waveplates, the laser is initially self-starting. After the mode-locking is initiated, the separation between filters can be tuned to obtain the broadest spectrum without losing mode-locking. As the spectral filters are adjusted to be apart, the cavity is not self-starting anymore.

To confirm the mode-locking mechanism, numerical simulations have been performed for the laser cavity described by cubic complex Ginzburg–Landau equation as

$$\frac{\partial U}{\partial t} = -i\frac{\beta_2}{2}\frac{\partial^2 U}{\partial t^2} + \frac{\beta_3}{6}\frac{\partial^3 U}{\partial t^3} + i\frac{\beta_4}{24}\frac{\partial^4 U}{\partial t^4} + \frac{g}{2}U + i\gamma|U|^2 U + i\gamma h_R \frac{\partial^2 U}{\partial t^2} U, \tag{1}$$

where $U = U(z,t)$ is the pulse envelope function; z is the propagation distance; t is the time; and β_2, β_3, and β_4 are the second-order (GVD), third-order, and fourth-order dispersion parameters, respectively. γ is the nonlinearity coefficient given by $\gamma = n_2\omega_0/cA_{\mathrm{eff}}$, where n_2 is the Kerr coefficient, ω_0 is the central angular frequency, c is the velocity of light in vacuum, A_{eff} is the effective mode area, and h_R is responsible for the self-frequency shift induced by intrapulse Raman scattering. The gain saturation is given by $g(E) = \frac{g_0}{1+E/E_{\mathrm{Sat}}}$, where E is the pulse energy given by $E = \int_{-T_R/2}^{T_R/2} |A(z,t)|^2 \mathrm{d}t$, T_R is the cavity round trip time, E_{Sat} is the saturation energy, and g_0 is the small signal gain. We use the following parameters for our simulations, which match the experimental conditions: $\gamma = 3.71\ \mathrm{W}^{-1}\cdot\mathrm{km}^{-1}$ for SMF, $\gamma = 4.83\ \mathrm{W}^{-1}\cdot\mathrm{km}^{-1}$ for YDF and $\gamma = 19.85\ \mathrm{W}^{-1}\cdot\mathrm{km}^{-1}$ for PCF, $\beta_2 = 22.2\ \mathrm{fs}^2/\mathrm{mm}$, $\beta_3 = 63.8\ \mathrm{fs}^3/\mathrm{mm}$ for SMF, $\beta_2 = 24\ \mathrm{fs}^2/\mathrm{mm}$, $\beta_3 = 59\ \mathrm{fs}^3/\mathrm{mm}$ for YDF, $\beta_2 = 3.7\ \mathrm{fs}^2/\mathrm{mm}$, $\beta_3 = -6.84\ \mathrm{fs}^3/\mathrm{mm}$, and $\beta_4 = 160\ \mathrm{fs}^4/\mathrm{mm}$ for PCF; the output coupler has a 80:20 coupling ratio.

3. RESULTS AND DISCUSSION

To understand the intracavity pulse evolution, we performed numerical simulations by the standard split-step Fourier method. The simulation results are summarized in Fig. 2. Figure 2(a) shows the evolution of the pulse duration and spectral BW (at −20 dB level). In the first arm, pulse duration and spectral BW do not change much initially in the passive SMF. However, the duration and the spectral BW start to grow

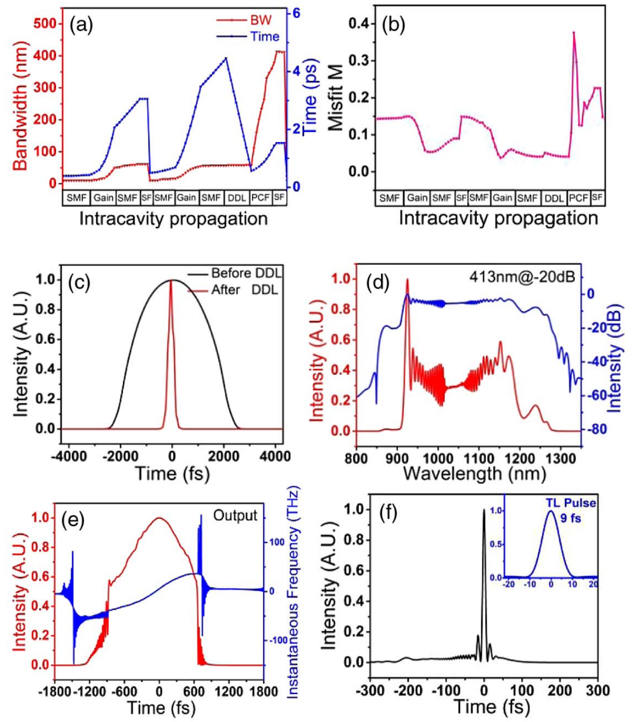

Fig. 2. (a) Pulse duration and spectral BW evolution in the laser cavity. (b) Misfit parameter M in the cavity. (c) Pulse before and after the DDL. (d) Output spectrum. (e) Output pulse. (f) Numerically dechirped pulse by a 300 lines/mm grating pair.

monotonically in the gain fiber and second passive SMF to form a positively chirped pulse. Figure 2(b) shows the evolution of the misfit parameter M to indicate the pulse shape. The misfit parameter, which shows how much the pulse profile deviates from a parabola, is defined as $M^2 = \int (I - I_{\mathrm{fit}})^2 \mathrm{d}t / \int I^2 \mathrm{d}t$, where I_{fit} is the pulse intensity profile, while I is the parabolic pulse intensity profile. For example, $M = 0.14$ is for a Gaussian pulse, while $M \leq 0.06$ corresponds to a parabolic pulse [28]. Figure 2(b) shows that the initial Gaussian pulse evolves to a parabolic pulse while propagating in the gain fiber, which is a key signature of the self-similar pulse evolution in normal GVD gain fibers [18,19]. The broadened self-similar spectrum is filtered by a sharp spectral filter (4 nm BW at 1050 nm) before the second arm.

In the second arm, the spectrum and the pulse durations broaden again in the gain fiber by the self-similar evolution, but the DDL reduces the pulse duration significantly from 4.5 ps to 560 fs [Fig. 2(c)]. Therefore, the pulse peak power is noticeably enhanced by ~8 times. While the compressed pulse is coupled into the PCF, the combination of the high peak power, small MFD, and small normal GVD induces a tremendous spectral broadening in the PCF. Over one round trip, the spectral BW broadens from 10 nm to 413 nm corresponding to a ~41 spectral breathing ratio. The broadened spectrum is coupled out of the cavity as an output [Figs. 2(d) and 2(e)] with 413 nm BW at −20 dB level below the peak.

Figure 2(f) shows the peak-power-optimized pulse profile (10 fs) after dechirping by a 300 lines/mm grating pair accounting for the GVD and the third-order dispersion (TOD) of the

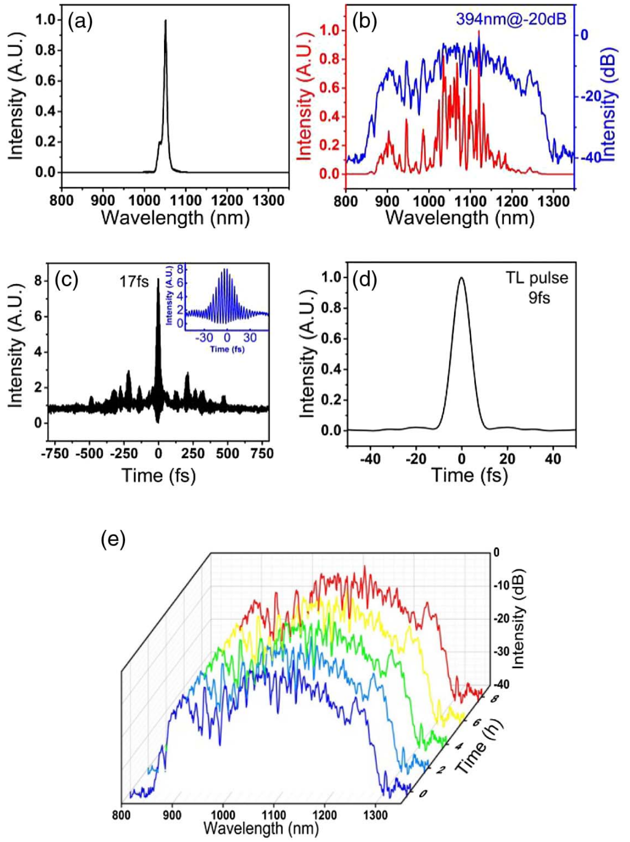

Fig. 3. Experimental results. (a) Output spectrum from the PBS1. (b) Output spectrum. (c) Dechirped autocorrelation. (d) Calculated Fourier transform limited pulse profile. (e) Output spectrum stability over an 8 h window.

grating pair. Even though the full width at half-maximum (FWHM) pulse duration is close to the Fourier transform limited pulse duration (~9 fs), a long pedestal is observed due to uncompensated higher-order dispersion effect. Since the third-order phase of the pulse and the TOD of the grating pair add up, it is important to suppress the TOD of the grating pair to improve the pulse duration. However, the simulations also indicate that the third-order phase of the pulse is so large that tuning the TOD of the grating pair does not improve the pulse duration significantly. After the output is coupled out of the cavity, a sharp spectral filter (4 nm BW at 1040 nm) again cuts down the spectrum before the pulse returns to the first arm.

The mode-locking is initiated at the pump thresholds of 490 mW and 514 mW for the two pumps by adjusting the wave plates. Figure 3(a) shows the ejected spectrum at PBS1, while Fig. 3(b) shows the output spectrum at the PBS2 when pump 1 and pump 2 reach 780 mW and 1.4 W, respectively. The average output power is 62 mW, and the pulse energy is 3.5 nJ at 17.5 MHz repetition rate with 394 nm BW at −20 dB. The autocorrelation [Fig. 3(c)] shows 17 fs (~5 cycles) pulse duration after dechirping by a 300 lines/mm grating pair. In the autocorrelation signal, noticeable pedestals are observed owing to uncompensated higher order GVDs by a grating pair. It is believed that Fourier transform limited pulses [~9 fs, Fig. 3(d)] can be obtained with a better phase compensation technique such as a multiphoton intrapulse interference phase scan (MIIPS) [29]. A chirped-mirror-based compression technique can be another alternative since chirped mirrors can be designed to compensate higher-order dispersions.

Figure 3(e) shows the spectral measurement recorded for eight consecutive hours. It can be inferred that the spectrum is stable even in a decibel scale for hours. However, the laser did not sustain its stability for more than a day due to the mechanical drift in the oscillator. For example, as the spectrum changes, once we tweak the position of the PCF, we can obtain the same broad spectrum. We strongly believe that this issue can be resolved by an all-fiber Mamyshev oscillator.

In the experiment, an anomalous DDL and a highly nonlinear ANDi PCF induced a huge spectral broadening. Of course, this explosive intracavity spectral broadening can disturb stable mode-locked operations. As mentioned in the introduction, there are two main mechanisms to stabilize the dramatic mode-locked operation. First, there is a strong nonlinear attractor action that is induced by a combination of the self-similar evolution in the gain fiber and a narrow spectral filtering. An ultrabroad spectrum is cut by a sharp spectral filter, but the BW grows again as it reaches the nonlinear attractor of the parabolic self-similar pulse. The nonlinear attraction action not only reestablishes a parabolic pulse profile but also cleans the complex nonlinear phase shift in the spectral broadening process.

Second is the "perfect" step-like saturable absorbing action of the Mamyshev regenerator. In fact, numerical simulations indicate that it is possible to obtain such a broad spectrum in a simple self-similar fiber laser [24]. However, the simulation could not generate such a broad spectrum unless almost an ideal saturable absorber with a very strong modulation depth (nearly 100%), which is rarely available in reality, is assumed in simulations. In contrast, it is verified in numerical studies and experiments that the Mamyshev oscillator can stabilize such operations, proving that the step-like saturable absorber is essential.

In the experiment, the pulse energy was limited to 3.5 nJ as part of the energy was lost in the free space coupling into PCF. We believe that pulse energy will improve with an all-fiber oscillator design. We also numerically investigated the generation of ultrabroadband high-energy pulses by increasing the pump power. Unfortunately, the simulation was unable to converge due to excessive perturbation. It is believed that further scaling of the energy is possible by employing large-mode-area fibers in a Mamyshev oscillator [27].

Further numerical studies show that we can generate even an octave spanning spectrum (632 nm at –20 dB), which is nearly a single-cycle (5 fs) pulse directly from the Mamyshev oscillator [Figs. 4(a) and 4(b)]. To obtain the octave spanning, the gain parameter has been modified to have more self-similar pulse energy before the PCF. It indicates that it is possible to generate nearly single-cycle pulses directly from fiber lasers by having a properly designed gain fiber, which will be a significant breakthrough for mode-locked fiber lasers in generating extremely short pulses.

In conclusion, we demonstrated ultrabroadband, few-cycle pulses directly from a Mamyshev fiber oscillator. The extreme spectral broadening in the cavity can be stabilized by the self-similar evolution and the perfect saturable absorber action of the Mamyshev oscillator. To the best of our knowledge, this is the broadest spectrum and shortest pulse (17 fs) directly generated from a mode-locked fiber laser.

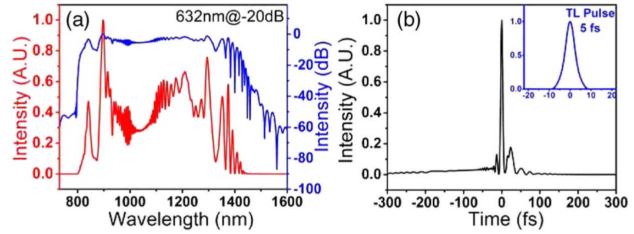

Fig. 4. Octave spanning simulation results. (a) Output spectrum. (b) A 300 lines/mm grating pair dechirped pulse and its Fourier transform limited pulse.

Funding. National Science Foundation (1710914); China Scholarship Council (201706170153).

Acknowledgment. We sincerely appreciate Professor Jonathan Knight at University of Bath for providing ANDi PCF for experiments.

Disclosures. The authors declare no conflicts of interest.

REFERENCES

1. D. A. Orringer, B. Pandian, Y. S. Niknafs, T. C. Hollon, J. Boyle, S. Lewis, M. Garrard, S. L. Hervey-Jumper, H. J. L. Garton, C. O. Maher, J. A. Heth, O. Sagher, D. A. Wilkinson, M. Snuderl, S. Venneti, S. H. Ramkissoon, K. A. McFadden, A. Fisher Hubbard, A. P. Lieberman, T. D. Johnson, X. S. Xie, J. K. Trautman, C. W. Freudiger, and S. Camelo-Piragua, "Rapid intraoperative histology of unprocessed surgical specimens via fibre-laser-based stimulated Raman scattering microscopy," Nat. Biomed. Eng. **1**, 0027 (2017).
2. K. Sugioka and Y. Cheng, "Femtosecond laser three-dimensional micro- and nanofabrication," Light Sci. Appl. **3**, e149 (2014).
3. C. M. Jewart, Q. Wang, J. Canning, D. Grobnic, S. J. Mihailov, and K. P. Chen, "Ultrafast femtosecond-laser-induced fiber Bragg gratings in air-hole microstructured fibers for high-temperature pressure sensing," Opt. Lett. **35**, 1443–1445 (2010).
4. M. Dantus, M. J. Rosker, A. H. Zewail, and J. Chem, "Real-time femtosecond probing of 'transition states' in chemical reactions," J. Chem. Phys. **87**, 2395–2397 (1987).
5. J. Ye, T. H. Yoon, J. L. Hall, A. A. Madej, J. E. Bernard, K. J. Siemsen, L. Marmet, J.-M. Chartier, and A. Chartier, "Accuracy comparison of absolute optical frequency measurement between harmonic-generation synthesis and a frequency-division femtosecond comb," Phys. Rev. Lett. **85**, 3797–3800 (2000).
6. T. Udem, J. Reichert, R. Holzwarth, and T. W. Hänsch, "Absolute optical frequency measurement of the cesium D1 line with a mode-locked laser," Phys. Rev. Lett. **82**, 3568–3571 (1999).
7. F. Calegari, G. Sansone, S. Stagira, C. Vozzi, and M. Nisoli, "Advances in attosecond science," J. Phys. B **49**, 062001 (2016).
8. M. Hentschel, R. Kienberger, C. Spielmann, G. A. Reider, N. Milosevic, T. Brabec, P. Corkum, U. Heinzmann, M. Drescher, and F. Krausz, "Attosecond metrology," Nature **414**, 509–513 (2001).
9. P. Villoresi, P. Ceccherini, L. Poletto, G. Tondello, C. Altucci, R. Bruzzese, C. de Lisio, M. Nisoli, S. Stagira, G. Cerullo, S. De Silvestri, and O. Svelto, "Spectral features and modeling of high-order harmonics generated by sub-10-fs pulses," Phys. Rev. Lett. **85**, 2494–2497 (2000).

10. C. Spielmann, N. H. Burnett, S. Sartania, R. Koppitsch, M. Schnürer, C. Kan, M. Lenzner, P. Wobrauschek, and F. Krausz, "Generation of coherent X-rays in the water window using 5-femtosecond laser pulses," Science **278**, 661–664 (1997).
11. U. Morgner, F. X. Kärtner, S. H. Cho, Y. Chen, H. A. Haus, J. G. Fujimoto, E. P. Ippen, V. Scheuer, G. Angelow, and T. Tschudi, "Sub-two-cycle pulses from a Kerr-lens mode-locked Ti:sapphire laser," Opt. Lett. **24**, 411–413 (1999).
12. D. H. Sutter, G. Steinmeyer, L. Gallmann, N. Matuschek, F. Morier-Genoud, U. Keller, V. Scheuer, G. Angelow, and T. Tschudi, "Semiconductor saturable-absorber mirror–assisted Kerr-lens mode-locked Ti:sapphire laser producing pulses in the two-cycle regime," Opt. Lett. **24**, 631–633 (1999).
13. R. Ell, U. Morgner, F. X. Kärtner, J. G. Fujimoto, E. P. Ippen, V. Scheuer, G. Angelow, T. Tschudi, M. J. Lederer, A. Boiko, and B. Luther-Davies, "Generation of 5-fs pulses and octave-spanning spectra directly from a Ti:sapphire laser," Opt. Lett. **26**, 373–375 (2001).
14. W. J. Tomlinson, R. H. Stolen, and C. V. Shank, "Compression of optical pulses chirped by self-phase modulation in fibers," J. Opt. Soc. Am. B. **1**, 139–149 (1984).
15. R. L. Fork, C. H. Brito Cruz, P. C. Becker, and C. V. Shank, "Compression of optical pulses to six femtoseconds by using cubic phase compensation," Opt. Lett. **12**, 483–485 (1987).
16. M. Nisoli, S. De Silvestri, O. Svelto, R. Szipöcs, K. Ferencz, C. Spielmann, S. Sartania, and F. Krausz, "Compression of high-energy laser pulses below 5 fs," Opt. Lett. **22**, 522–524 (1997).
17. G. Krauss, S. Lohss, T. Hanke, A. Sell, S. Eggert, R. Huber, and A. Leitenstorfer, "Synthesis of a single cycle of light with compact erbium-doped fibre technology," Nat. Photonics **4**, 33–36 (2010).
18. W. H. Renninger, A. Chong, and F. W. Wise, "Self-similar pulse evolution in an all-normal-dispersion laser," Phys. Rev. A. **82**, 021805 (2010).
19. B. Oktem, C. Ülgüdür, and F. Ö. Ilday, "Soliton–similariton fibre laser," Nat. Photonics **4**, 307–311 (2010).
20. C. Aguergaray, D. Méchin, V. Kruglov, and J. D. Harvey, "Experimental realization of a mode-locked parabolic Raman fiber oscillator," Opt. Express **18**, 8680–8687 (2010).
21. M. E. Fermann, V. I. Kruglov, B. C. Thomsen, J. M. Dudley, and J. D. Harvey, "Self-similar propagation and amplification of parabolic pulses in optical fibers," Phys. Rev. Lett. **84**, 6010–6013 (2000).
22. A. Chong, L. G. Wright, and F. W. Wise, "Ultrafast fiber lasers based on self-similar pulse evolution: a review of current progress," Rep. Prog. Phys. **78**, 113901 (2015).
23. A. Chong, H. Liu, B. Nie, B. G. Bale, S. Wabnitz, W. H. Renninger, M. Dantus, and F. W. Wise, "Pulse generation without gain-bandwidth limitation in a laser with self-similar evolution," Opt. Express **20**, 14213–14220 (2012).
24. A. Khanolkar, C. Ma, and A. Chong, "Generation of octave spanning spectra directly from a fiber oscillator with self-similar pulse evolution," in *Conference on Lasers and Electro-Optics* (Optical Society of America, 2018), paper JTh2A.111.
25. Z. Liu, Z. M. Ziegler, L. G. Wright, and F. W. Wise, "Megawatt peak power from a Mamyshev oscillator," Optica **4**, 649–654 (2017).
26. S. Pitois, C. Finot, L. Provost, and D. J. Richardson, "Generation of localized pulses from incoherent wave in optical fiber lines made of concatenated Mamyshev regenerators," J. Opt. Soc. Am. B **25**, 1537–1547 (2008).
27. W. Liu, R. Liao, J. Zhao, J. Cui, Y. Song, C. Wang, and M. Hu, "Femtosecond Mamyshev oscillator with 10-MW-level peak power," Optica **6**, 194–197 (2019).
28. X. Li, S. Zhang, and Z. Yang, "Optimal design of similariton fiber lasers without gain-bandwidth limitation," Opt. Express **25**, 18410–18420 (2017).
29. V. V. Lozovoy, I. Pastirk, and M. Dantus, "Multiphoton intrapulse interference. IV. Ultrashort laser pulse spectral phase characterization and compensation," Opt. Lett. **29**, 775–777 (2004).